Journal of Supramolecular Structure 5:155 (107)–183 (135) (1976)

Localization and Organization of Microfilaments and Related Proteins in Normal and Virus-Transformed Cells

Robert D. Goldman, Marie-Jeanne Yerna, and Jeffery A. Schloss

Department of Biological Sciences, Mellon Institute of Science, Carnegie-Mellon University, Pittsburgh, Pennsylvania 15213

The localization and organization of actin-like microfilaments in normal, SV-40 and adenovirus transformed cells are determined by the coordinated use of light optical, electron optical and biochemical techniques. In adenovirus-type 5 transformed hamster embryo cells, microfilament meshworks appear to be the predominant organizational form of cellular actin, while in normal hamster cells, microfilament bundles are prevalent. Differences between 3T3 and SV-40 transformed 3T3 cells are less apparent and may be related to the packing and intracellular distribution of microfilament bundles. Attempts at relating these ultrastructural changes in transformed cells to the images obtained following reaction with fluorescein-labelled myosin fragments and indirect immunofluorescence with smooth muscle myosin antibody are discussed. In several instances the fluorescence microscope images do not correspond to the ultrastructural observations. The results are discussed in terms of the possible relationships between alterations in cytoplasmic contractile elements and the abnormal behavior of transformed cells.

Key words: microfilaments, actin, myosin, transformed cells

INTRODUCTION

Microfilaments are found in the cortical cytoplasm of animal cells (1–3). They are considered to be the major nonmuscle form of actin due to their size (~ 5 nm; 2), interaction with rabbit muscle heavy meromyosin (HMM) and subfragment-1 (S-1) (2–5), and the fact that a protein almost identical to muscle actin has been isolated from many types of animal cells (6). Due to their close proximity with the plasma membrane, microfilaments are thought to be involved in many cell surface activities, which include membrane ruffling and contact inhibition (7, 8), cytokinesis (9, 10), locomotion (2, 8), and microspike activity (11).

Microfilaments are found in several organizational forms in interphase cells as determined by electron microscopy. The most extensively studied of these forms are microfilament bundles (mfb) (1–3, 8, 12–16), which consist of tightly packed parallel arrays of

microfilaments. Under optimal conditions, these bundles can be visualized as "stress fibers" in extensively flattened living cells (1, 8, 12, 16). Other microfilament configurations have also been described and are termed microfilament meshworks (3, 8) and microfilament networks (14–15, 17–19). Electron microscopic studies of suspended cells and cells in the process of attachment to and spreading on solid substrates have led to the suggestion that microfilament meshworks and microfilament bundles may be interconvertible and that the formation and loss of cell-cell and cell-substrate contacts signals these interconversions (3, 8, 12).

Recent light microscopic studies utilizing the technique of indirect immunofluorescence with actin antibody have provided evidence that confirms that stress fibers which correspond to microfilament bundles contain actin-like protein (16, 20). Similar studies have suggested that stress fibers also contain proteins similar to myosin, α-actinin, and tropomyosin (20–26). Therefore, it appears as if stress fibers may represent an organized form of an actomyosin-like contractile system. This system is probably involved in cortical contractility, which in turn may be directly responsible for motile activities associated with the cell surface.

A major benefit of the immunofluorescence procedures is that in certain cases they can provide a rapid overview of the distribution of protein structures related to cell motility, without the necessity of prolonged ultrastructural analysis. The technique has been exploited successfully in selected cells that display an obvious relationship between stress fibers and microfilament bundles (16). The results of these studies have provided new insight into the possibility that contractile proteins other than actin may be localized within microfilament bundles (20–26). One of the major drawbacks of the fluorescence technique is the limited resolving power of fluorescence microscopy relative to electron microscopy. For example, one cannot determine the molecular arrangements or orientation of microfilaments within mfb by fluorescence microscopy alone and therefore it is necessary to correlate fluorescence images with the electron images obtained from thin sectioned cells (16).

Electron microscopy has been used to suggest that there are fewer actin-like microfilament bundles in SV40 transformed mouse 3T3 cells (27–28) and in human adenovirus-5 transformed hamster cells (29), relative to the normal cells from which they are derived. However, no attempts have been made to quantitate these possible differences in the number of microfilament bundles. More recently, immunofluorescence techniques have been used to show that stress fibers or "sheaths" containing actin-like and myosin-like proteins are reduced in number or are missing in some types of SV40 transformed cells (30–32). Since diffuse fluorescence is present in these cells, it has been suggested that actin is in some way rearranged in the cytoplasm (31).

In this study we review our past and more recent efforts to use coordinated light and electron microscopic methods to further elucidate and quantitate the differences in actomyosin-like proteins seen in normal and transformed cells. The overall results demonstrate that there are significant alterations in the distribution and organization of these proteins in transformed cells that may be related to their altered behavior. The results also demonstrate that in some instances the fluorescence techniques produce images that correspond with the subcellular organization of microfilament bundles and in other instances there is no such correspondence.

MATERIALS AND METHODS

Cell Cultures

Rat embryo cells (obtained from 18- to 20-day-old trypsinized-dissociated embryos), mouse 3T3 cells, SV40 transformed 3T3 cells (line SV101,* a gift of Dr. Robert Pollack), normal hamster embryo cells (line 9; Ref. 33), and adenovirus-5 transformed 9 cells (line 14b (Ref. 33) were grown in Dulbecco's Modified Eagle's Medium (GIBCO) containing 10% calf serum. Stock cultures of all cells were kept at 37°C in a CO_2 incubator. These stocks were subcultured by treatment with 0.05% trypsin-ethylenediaminetetraacetate solution (GIBCO). Cells were grown on 22 mm^2 No. 1 glass coverslips for light microscopy and on 35 or 60 mm diameter Falcon plastic tissue culture dishes for electron microscopy.

Light Microscopy

Coverslips containing cells were mounted on 1 mm glass slides as described previously (34). All photomicrographs were taken with a Zeiss Photomicroscope III equipped with phase contrast, Nomarksi differential interference and IIIRS epifluorescence optics. Unless otherwise noted, fluorescence micrographs were taken with Zeiss 40X Neofluor (N.A. 0.75), 40X oil immersion apochromat (N.A. 1.0), and 100X oil immersion planachromat (N.A. 1.25) objectives on Plus-X film. Phase contrast and Nomarksi photomicrographs were taken on Panatomic-X film. Both types of film were developed with Diafine two-stage developer.

Immunofluorescence

Cells on coverslips were fixed in 3.7% formaldehyde in phosphate-buffered saline (PBS) for 10–20 min (at room temperature), rinsed 3 times in PBS, extracted with cold acetone (−20°C) for 1–2 min, and then air dried; 20 μl of antiserum (1:10 dilution in PBS) was placed on the cells and the coverslip was incubated for 30–60 min at 37°C in a humidified chamber. The coverslips were then rinsed in PBS (3–5 times) and incubated in goat antirabbit IgG labeled with fluorescein (Miles-Yeda) that had been purified on a DEAE-cellulose ion exchange column.

The rabbit antiserum used was directed against column-purified chicken gizzard myosin (a gift of Dr. David Hartshorne). This protein was over 95% pure as determined by sodium dodecyl sulfate (SDS) disc gel electrophoresis. The specificity of the antiserum was determined by an Ouchterlony two-dimensional double-immunodiffusion assay. Only one precipitin band was detected between the antiserum and the antigen. No precipitin band was seen between the antiserum and preimmune serum taken from the same rabbit.

The staining of stress fibers observed appeared identical to that seen by others who have used smooth muscle myosin antibody on similar types of cells (e.g., 21). Preimmune serum controls showed barely perceptible fluorescence and no stress fibers were apparent.

HMM and S-1 Binding

Rabbit skeletal muscle myosin was prepared according to the technique of Szent-Györgyi (35). The heavy meromyosin (HMM) and subfragment-1 (S-1) used were prepared by digestion with α-chymotrypsin (Sigma bovine 3X cryst.) according to the technique of Weeds and Taylor (36). HMM was also prepared by digestion with trypsin (37).

*All SV101 cells utilized in these studies were T-antigen positive, as determined by indirect immunofluorescent staining of subconfluent coverslip cultures (antiserum kindly provided by Dr. James McDougall).

Fluorescein labeled S-1 and HMM (FS-1, FHMM) were prepared by slight modifications of Aronson's technique (38). It was found that 70% of the actin-activatable ATPase activity was retained following conjugation of S-1 with fluorescein isothiocyanate (FITC). Details regarding the preparation and use of FHMM and FS-1 are included in a paper that has been submitted to the Journal of Cell Biology (Goldman, R. D., Schloss, J. A., Yerna, M-J., and Forer, A., 1976).

The glycerination procedure used for detecting HMM, S-1, FHMM, and FS-1 binding by both fluorescence and electron microscopy has been described in detail elsewhere (3).

Electron Microscopy

Cells on plastic dishes were fixed at room temperature for 15–60 min in 1% glutaraldehyde in PBS, rinsed in PBS, and postfixed for 15–60 min in 1% osmium tetroxide in PBS. Details of the procedures for fixing and flat-embedding cultured cells with and without prior glycerination have been described elsewhere (34). In all cases small pieces were cut from the disc of plastic containing cells that was removed from petri dishes (34). These pieces were glued on the ends of prepolymerized Epon blocks made in BEEM capsules. The block faces were trimmed to ~ 0.5 mm^2, and silver-gold sections were cut parallel to the substrate of flat-embedded cells on a diamond knife mounted in an LKB Ultrotome. The sections were collected on Formvar-carbon coated grids and stained with uranyl acetate (40) and lead citrate (41). Electron micrographs were taken on Kodak electron image film with a Philips 201C electron microscope.

Gel Electrophoresis

An estimation of the amount of protein in 9 and 14b cells that comigrated with purified skeletal muscle actin was obtained from densitometric traces of SDS gels. Five 100 mm Falcon culture dishes of both 14b and 9 cells were washed several times with PBSa (Ca^{++}-Mg^{++}-free). The cells were then removed with a rubber policeman in a final volume of 3.5 ml of 10 mM Tris-HCl (pH 7.5) containing 0.5 ml of phenylmethyl sulfonyl fluoride (0.7% solution in 95% ethanol). Each of these cell samples was sonicated and the resulting suspension was dialyzed for 3 hr against 10 mM Tris-HCl (pH 7.5). The amount of protein in each sample was determined by the Biuret method. By the method of Fairbanks et al. (39), 15, 25, and 40 μg aliquots of protein from each cell type were subjected to SDS polyacrylamide gel electrophoresis at 6 mA per gel. The gels were then stained with Coomassie brilliant blue R and scanned in a Beckman spectrophotometer.

RESULTS

Correspondence Between Stress Fibers and Microfilament Bundles in Embryonic Cells

There are many extensively flattened or spread cells in cultures obtained from dissociated 18- to 20-day-old rat embryos (RE cells). These cells are useful for studying and determining the properties of stress fibers by light and electron microscopy (1, 8, 30–32). Stress fibers within living cells of this type are easily visualized by phase contrast (Fig. 1), and Nomarski differential interference optics. Observations with this latter technique have revealed that the majority of stress fibers are distributed towards the adhesive surface of cells grown on glass coverslips (8).

When similar RE cells are extracted with glycerol for short time periods at room temperature (3), the stress fibers seen in living cells are preserved in extracted cells (Figs. 2A and 2B). This extraction procedure makes the cells permeable to large molecules such

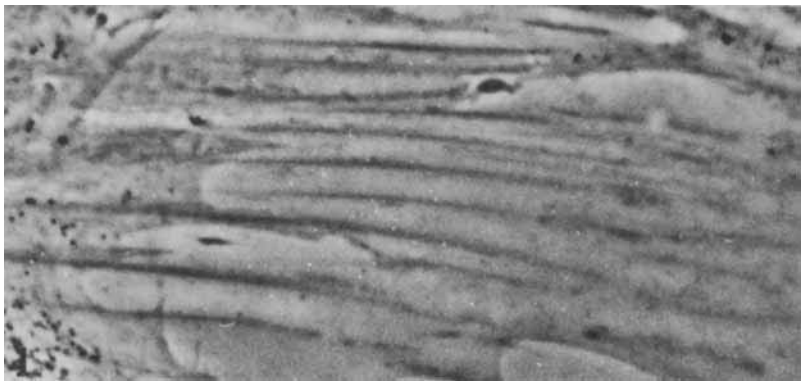

Fig. 1. Part of an extensively flattened living RE cell displaying stress fibers. Phase contrast, × 832.

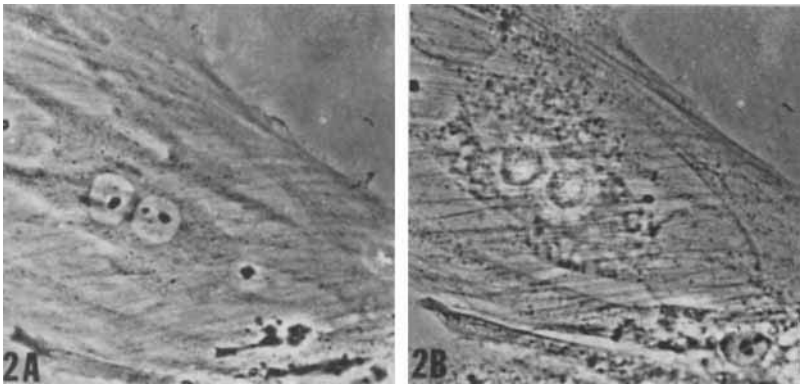

Fig. 2. A. Living RE cell. B. The same cell following glycerination (3). Most of the stress fibers seen in the living cell are preserved in the glycerinated cell. Stress fibers appear more prominent following glycerination, which may reflect a higher refractive index difference between stress fibers and surrounding cytoplasm due to the large amount of protein solubilized by this procedure (8). Phase contrast, × 416.

as FS-1 and FHMM. A glycerinated RE cell with an extensive array of fluorescent stress fibers following treatment with FS-1 is seen in Fig. 3. This is very similar to the pattern of stress fibers seen following treatment with actin antibody in similar cells (23, 31–32). Fluorescent stress fibers are also seen by immunofluorescence utilizing smooth muscle myosin or platelet myosin antibody (21–22). Figures 4A and 4B show the same cell as it appears in phase contrast and epifluorescence optics to demonstrate the coincidence of phase dense and fluorescent stress fibers. Figure 5 contains a region of an RE cell showing the periodic fluorescence that has been reported by others with similar preparations of smooth muscle myosin antibody (21). These observations indicate that stress fibers contain actin-like and myosin-like protein.

Ultrastructural observations of thin sections of flat-embedded RE cells show that bundles of ~ 5 nm microfilaments are located in the cortex adjacent to the adhesive surface of spread cells (Fig. 6) (also see 1, 3, 8, 12, 16). These correspond to the stress fibers seen by light microscopy (8, 16). Microfilament bundles are preserved during glycerol

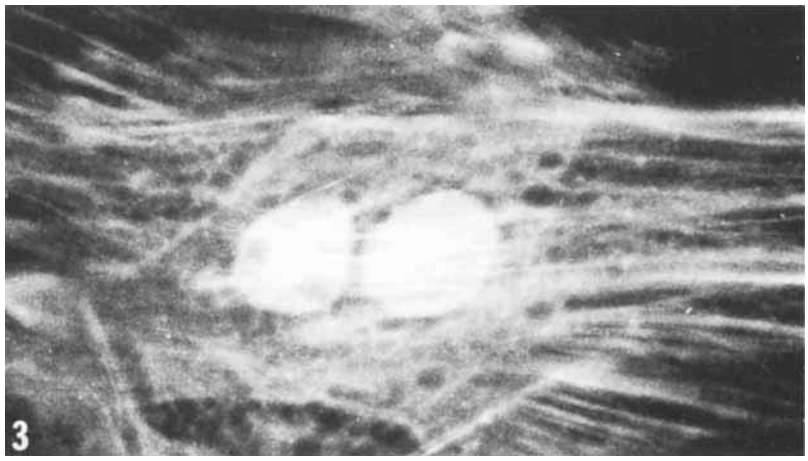

Fig. 3. Glycerinated RE cell treated with FS-1 for 15 min at room temperature and washed in standard salt solution (3). Fluorescent stress fibers are apparent. The image obtained is similar to that described by Sanger (43) following a similar procedure. Epifluorescence, × 832.

extraction (Fig. 7A) and are decorated following treatment with HMM or S-1 (Fig. 7B), demonstrating at the ultrastructural level that they are similar to muscle F-actin (8, 16).

In order to determine whether or not there is always a correspondence between stress fibers detected by light microscopy and microfilament bundles seen with electron microscopy, partially spread RE cells were studied. A large number of partially spread RE cells are easily obtained at 15–30 min following trypsinization and replating. Figure 8A is of a rat embryo cell 30 min following plating onto a glass coverslip. Stress fibers are not seen in these cells utilizing phase contrast or Nomarksi optics equipped with oil immersion objectives (numerical apertures 1.25–1.40). Such partially spread cells observed following processing for myosin antibody localization display no obvious fluorescent stress fibers, although they do exhibit intense peripheral fluorescence (Fig. 8B). Similar images are obtained following glycerination and reaction with FS-1.

Electron microscopic examination of flat-embedded rat embryo cells fixed at 30 min following plating reveals numerous microfilament bundles in the cortical cytoplasm adjacent to the adhesive surface of cells (Fig. 9). Submembranous areas of the cell surface not in contact with the substrate contain disorganized arrays of microfilaments known as microfilament meshworks (Figs. 10 and 10A) (3, 8). These meshworks are also present following glycerination, and microfilaments comprising the meshworks are seen to bind HMM (see Figs. 18A and 18B) (3, 8). Therefore, there is no obvious correspondence between the results obtained by light and electron microscopy with respect to microfilament bundles in slightly spread cells.

Differences in Microfilament Organization in Normal Hamster Embryo Cells and Their Human Adenovirus-5-Transformed Derivatives

A line of normal hamster embryo cells (line 9; Ref. 33) appears morphologically similar to rat embryo cells (Fig. 11A) (29). Stress fibers are apparent in most of the well-spread cells seen in growing cultures but are not apparent in partially spread or dividing cells in the same cultures (Fig. 11B). Stress fibers show intense fluorescence following the glycerination-FS-1 and myosin antibody staining procedures (Figs. 12A and 12B). When

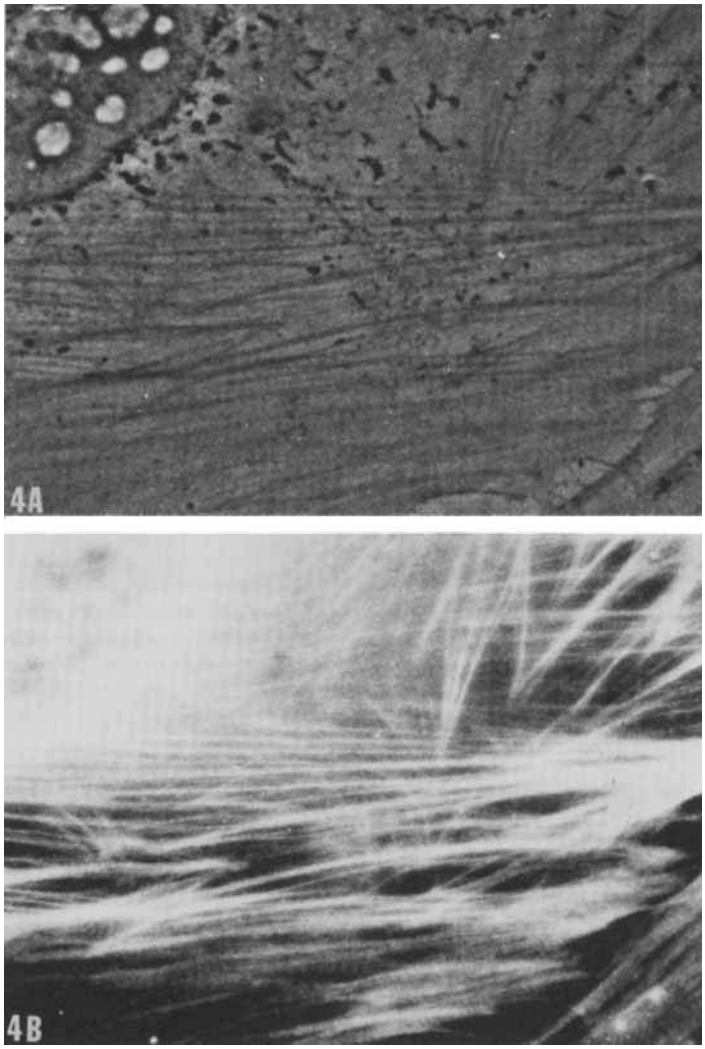

Fig. 4. RE cell fixed and prepared according to the myosin antibody procedure. The same cell viewed by phase contrast (A) and epifluorescence (B) optics. Note coincidence of phase-dense and fluorescent stress fibers, × 730.

thin sections of flat-embedded 9 cells are cut parallel to the substrate at the level of cell-substrate contact, extensive arrays of microfilament bundles are seen in all cells except for those engaged in mitosis (Fig. 13) (29).

Adenovirus-5-transformed derivatives of 9 cells (line 14b) are incapable of spreading normally on solid substrates (29). In subconfluent cultures ~ 80% of the cells remain rounded, show active surface blebbing but no membrane ruffling, and do not engage in locomotory behavior (Figs. 14A and 14B) (29). Stress fibers have not been seen in any living 14b cells. When they are examined following the FS-1 or myosin antibody procedures, no fluorescent stress fibers are seen. However, general fluorescence is seen throughout the cytoplasm with FS-1, and brighter regions are seen at the periphery with the antibody technique (Figs. 15A and 15B).

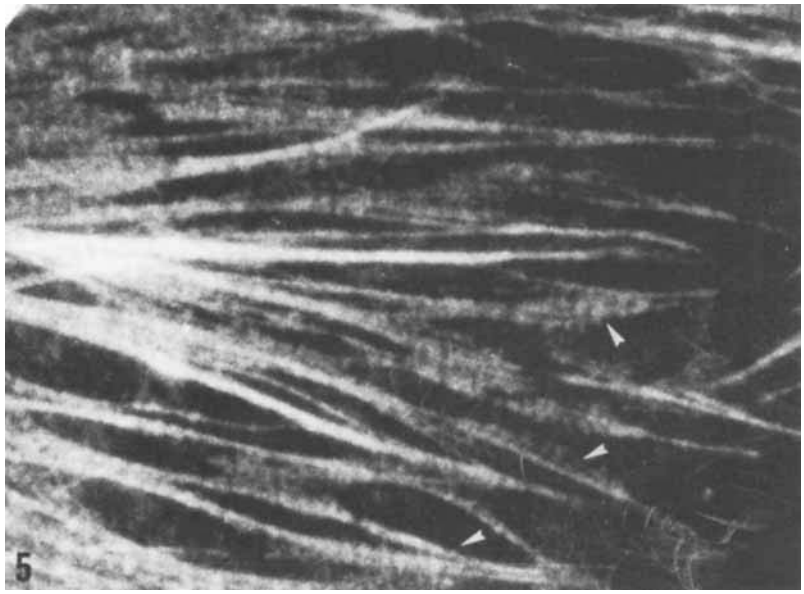

Fig. 5. Region of an RE cell containing stress fibers with periodic fluorescence (arrows) following a myosin antibody staining procedure. Not all cells display this feature as distinctly as this one. In addition, some cells contain periodically arranged fluorescent regions not associated with obvious stress fibers as determined by phase contrast microscopy. Epifluorescence, × 2,080.

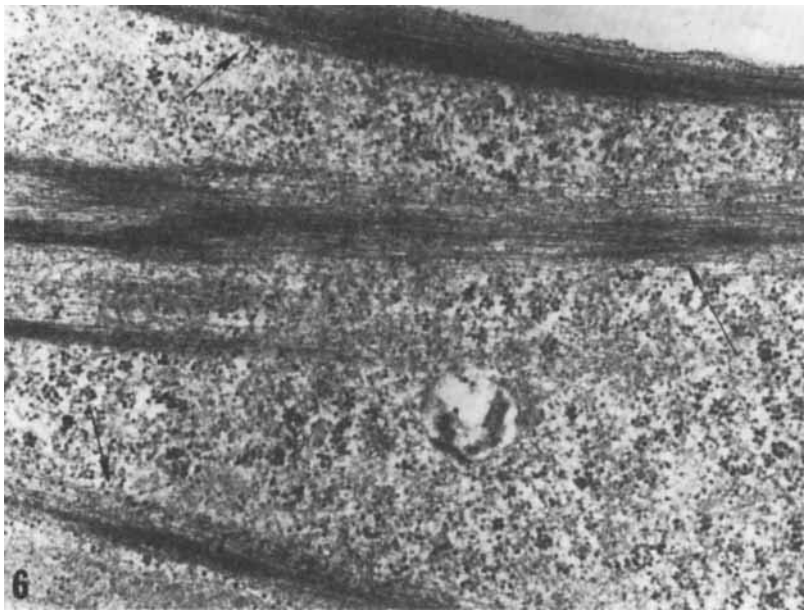

Fig. 6. Electron micrograph of a thin section made parallel to the substrate of a flat-embedded RE cell. The microfilament bundles (arrows) lie just beneath the plasma membrane in the cortex adjacent to cell-substrate contacts, × 32,000.

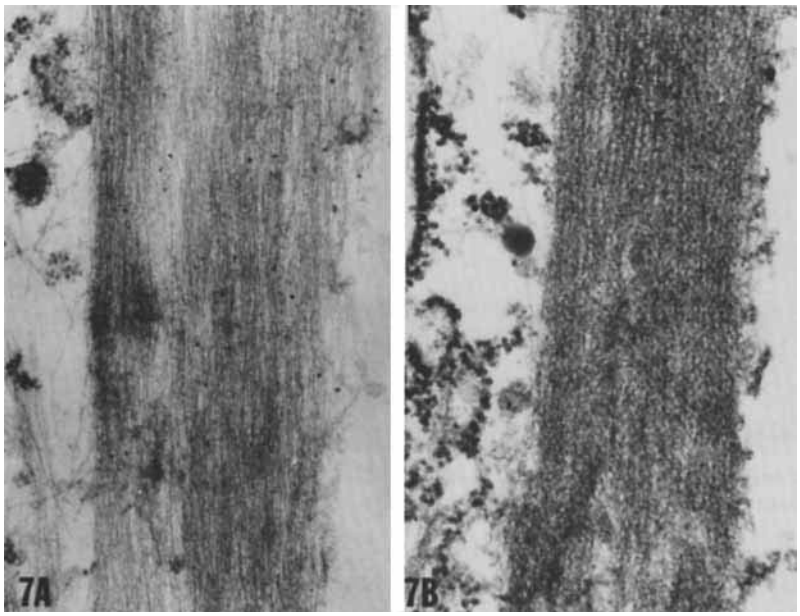

Fig. 7. A. Part of a microfilament bundle in a glycerinated RE cell as in Fig. 6. B. Part of a microfilament bundle in a glycerinated RE cell treated with HMM. Individual microfilaments appear thicker and more electron-dense and in some regions can be seen to possess a fuzzy appearance due to the outward projection of HMM molecules. Arrowheads are rarely seen within decorated microfilament bundles of this type. A) × 32,000; B) × 52,800.

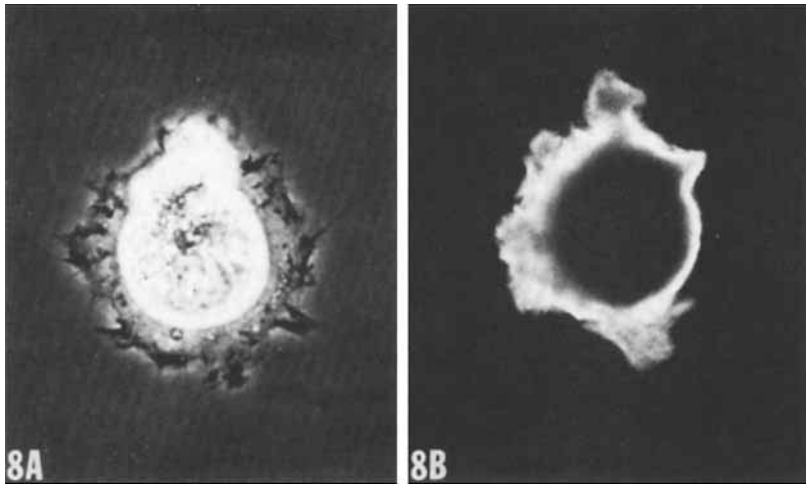

Fig. 8. A. Living RE cell observed at 30 min following plating. Ruffled membranes are present at the cell periphery. B. Similar RE cell prepared by the myosin antibody procedure. Areas containing ruffled membranes show intense fluorescence. A) Phase contrast, × 575; B) epifluorescence, × 1,040.

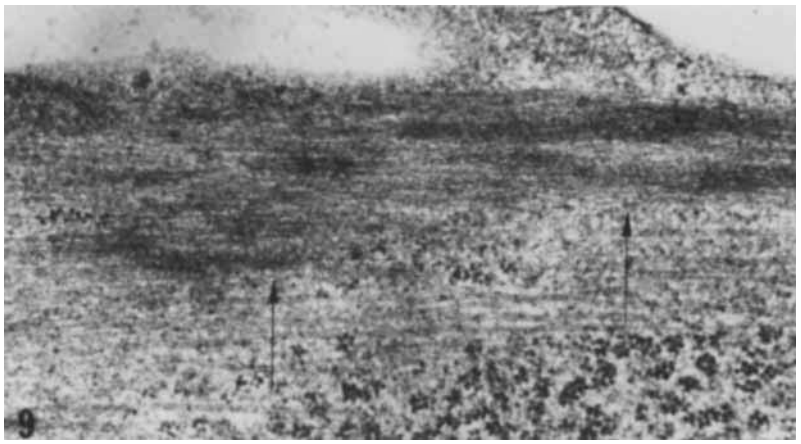

Fig. 9. A microfilament bundle (arrows) in an RE cell fixed and embedded at 30 min following plating onto a plastic culture dish. × 36,000.

Electron microscopic examination of subconfluent cultures of 14b cells demonstrate that the vast majority of cells lack microfilament bundles. Attempts made to quantitate the difference in microfilament bundles in 9 and 14b cells by counting bundles in sets of thin sections cut from the adhesive to the nonadhesive surface of both cell types are presented in Table I.

Although microfilament bundles are extremely rare in subconfluent cultures of 14b cells (Table I), there is a significant amount of actin-like protein that comigrates with purified skeletal muscle actin on SDS gel electrophoresis profiles (Fig. 16). The gel scans indicate that ~ 5.5% of total 14b cell protein and ~ 7.5% of total 9 cell protein comigrates with muscle actin (Fig. 16). Therefore, actin-like protein is abundant in 14b cells that lack microfilament bundles. However, ultrastructural analysis of the cortical region of 14b cells indicates that microfilament meshworks are present beneath the plasma membrane (Figs. 17 and 17A). This configuration is similar to that seen near the surface of spreading rat embryo cells not in contact with the substrate (see Figs. 10 and 10A) and in suspended BHK-21 and 3T3 cells (3, 8). The actin-like nature of the microfilaments included in this meshwork is evident following glycerination and HMM or S-1 binding (Figs. 18A and 18B).

The possibility that actin-like microfilament meshworks or other configurations known as microfilament networks (17–19) might represent grossly altered actin filaments induced by postfixation with osmium tetroxide has been suggested by Szamier and coworkers (42). We have investigated this possibility by fixing purified rabbit skeletal muscle F-actin with both glutaraldehyde and osmium tetroxide for time intervals that are similar to those used for fixing cells. The fixation solutions were identical to those used for cells, and the F-actin was treated on electron microscope grids for 30 min with glutaraldehyde and 15 min with osmium tetroxide and then examined by negative staining (Figs. 19A–19C). Actin filaments retain their overall structure following this fixation schedule, although in some cases they do appear somewhat wavier after treatment with osmium tetroxide (Fig. 19C). Cells fixed following an identical scheme contain both microfilament bundles and meshworks and are indistinguishable from cells fixed for 30–60 min in each of the solutions.

Szamier et al. (42) have also shown that actin decorated with HMM is protected from the structural alterations induced by osmium tetroxide. Since HMM or S-1 binding

to intracellular microfilaments takes place before fixation (3), decorated microfilaments in situ should be resistant to possible structural alterations induced by osmium tetroxide. Thus the observations that meshworks are present in glycerinated cells that have not been treated with HMM, and in those that have been treated with HMM, also support the

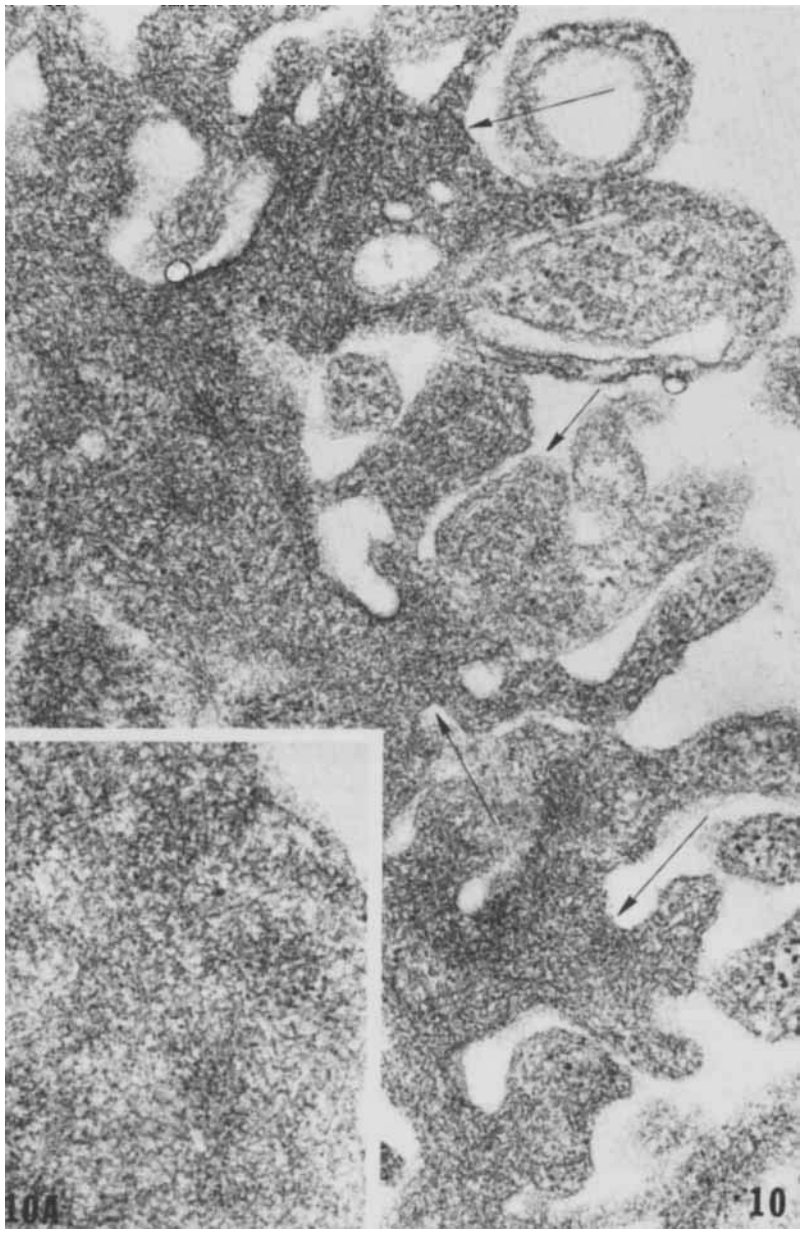

Fig. 10. Thin section showing the submembranous region (of an RE cell) not in contact with the substrate. The cortical cytoplasm contains disorganized arrays of microfilaments termed meshworks (arrows). Surface blebbing is seen frequently at the surface not in contact with the substrate and this explains the highly folded and convoluted appearance of the surface. A) Higher-magnification view of a microfilament meshwork. 10) × 52,000; 10A) × 66,000.

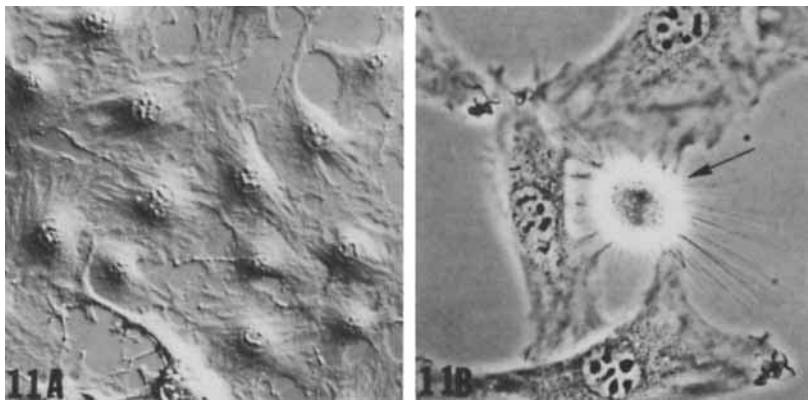

Fig. 11. A. Living 9 cells. B. A 9 cell rounding up for mitosis (arrow). The retraction fibers are completely resorbed prior to metaphase. A) Nomarksi, × 189; B) phase contrast, × 650.

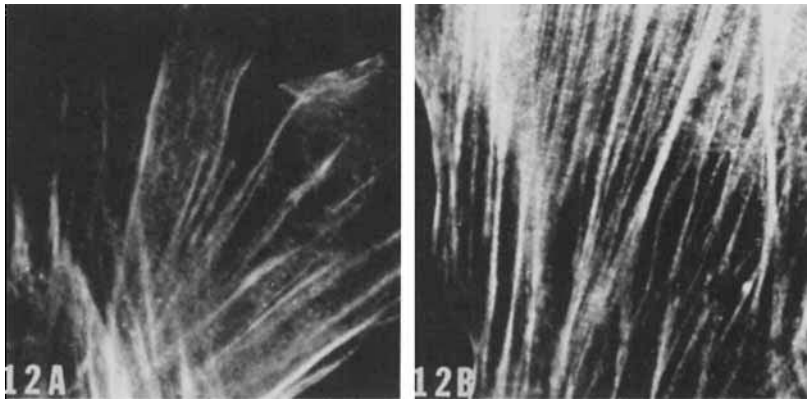

Fig. 12. A. A region of a well-spread 9 cell showing fluorescent stress fibers following glycerination and treatment with FS-1 for 15 min. B. A region of a well-spread 9 cell showing fluorescent stress fibers following the myosin antibody procedure. A) Epifluorescence, × 1,040; B) epifluorescence, × 1,040.

idea that the meshworks are another organizational state of intracellular microfilaments (Figs. 18A and 18B). Of course, the possibility that artifacts are produced by deleterious treatments inherent in processing cells for transmission electron microscopy cannot be ruled out completely.

Since 14b cells induce tumors rather easily and reproducibly in weanling hamsters (2–3 weeks old) (33), it is relevant to determine whether a similar lack of microfilament bundles is seen within the cells comprising such tumors. Ultrastructural studies of tumors excised and fixed for electron microscopy 4 weeks following the subcutaneous injection of 14b cells reveal that individual cells within the tumors possess a remarkable similarity to 14b cells grown in vitro. No submembranous microfilament bundles have been seen in any of the preparations examined so far. Microfilament meshworks have been detected in cortical regions. Therefore, 14b-induced tumors contain cells with arrays of microfilaments similar to those seen in 14b cells grown in vitro (Figs. 20A and 20B).

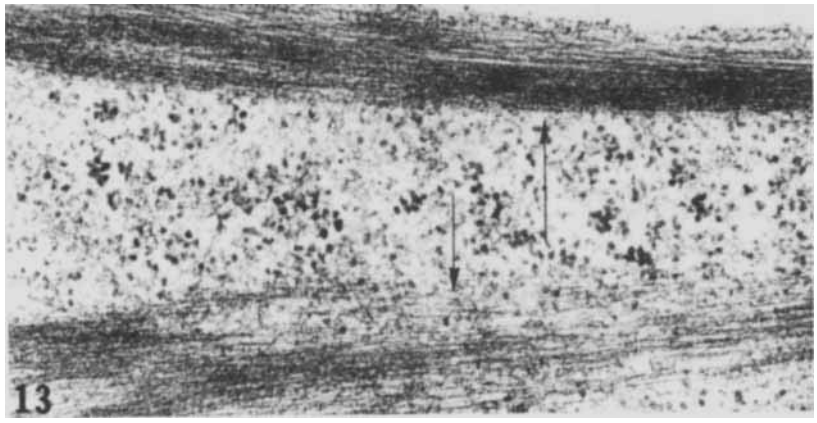

Fig. 13. An electron micrograph of a thin section cut parallel to, and at the level of, cell-substrate contact. Microfilament bundles are present (arrows), × 48,000.

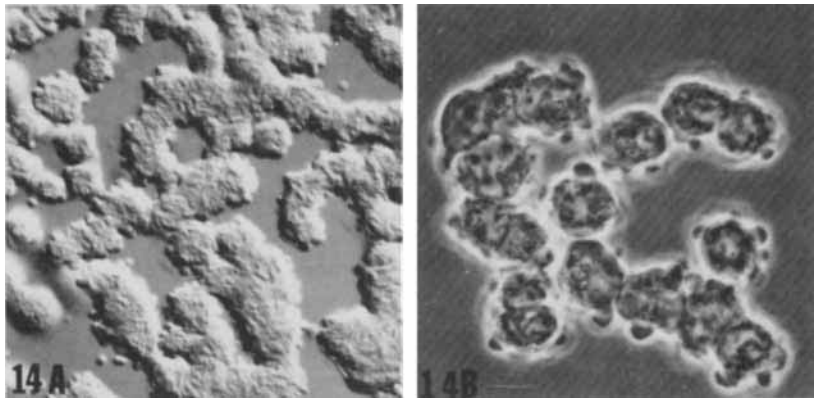

Fig. 14. Nomarski (A) and phase contrast (B) photomicrographs of living 14b cells. Note surface blebbing. A) × 255; B) × 800.

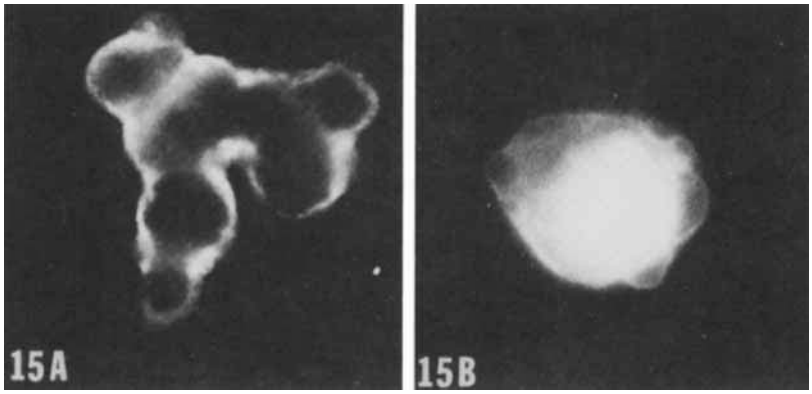

Fig. 15. A. 14b cells following the myosin antibody procedure. B. 14b cells following the FS-1 procedure. A) Epifluorescence, × 880; B) epifluorescence, × 1,520.

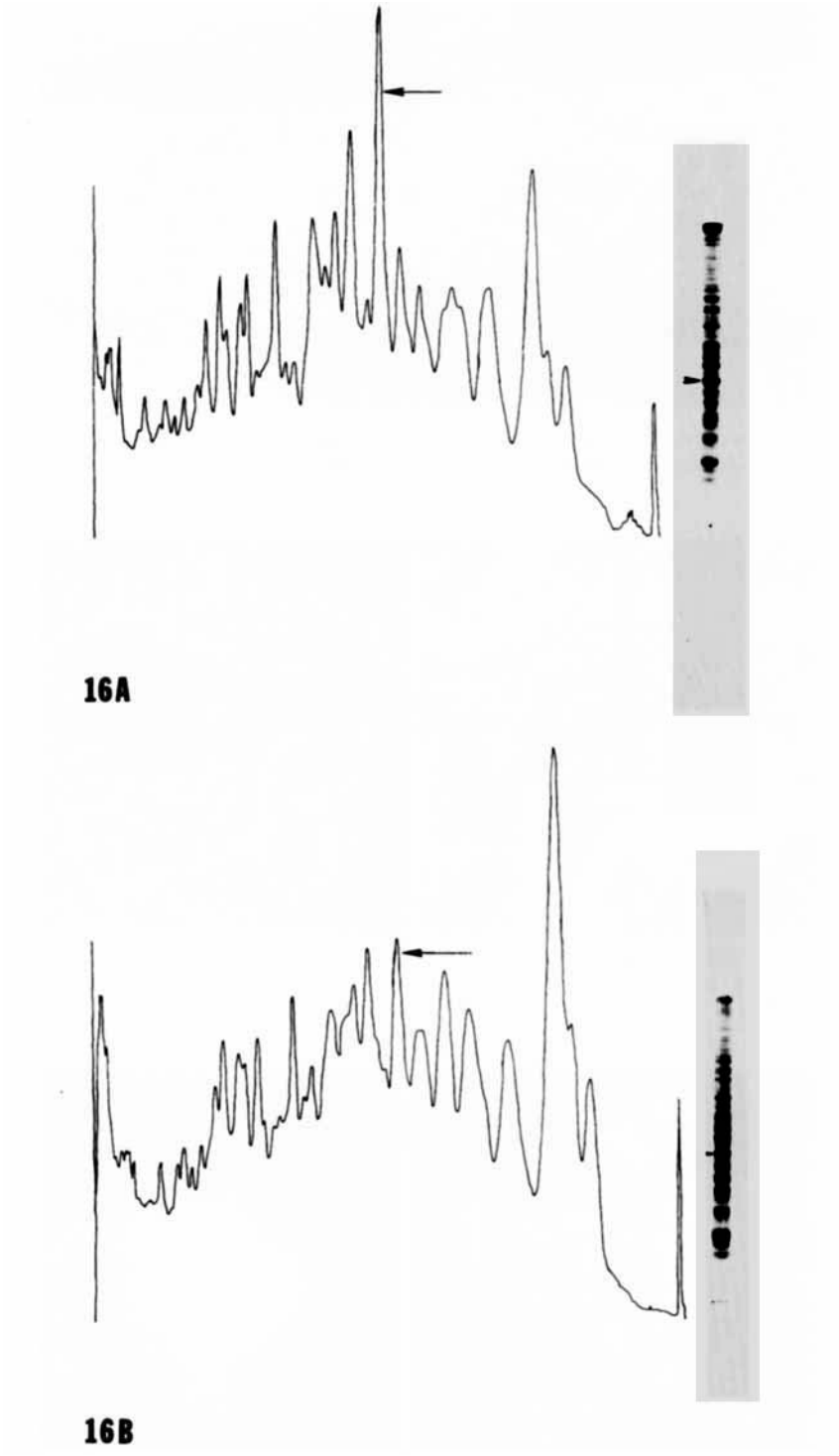

Fig. 16. SDS gels and scans of 9 (A) and 14b (B) cell protein (see Methods). Arrows point to bands which comigrate with purified skeletal muscle actin. The gels contain 15 μg of protein.

TABLE I. Microfilament Bundles in Sets* of Thin Sections of 9 and 14b Cells

Cell type	Total no. of cell profiles† per set of thin sections	Total no. of microfilament bundles per set of thin sections	Mean no. of microfilament bundles per cell profile
9	257	1,991	7.7
9	109	1,316	12.1
14b	372	7	0.02
14b	163	0	0

*A set of thin sections consisted of all the sections made parallel to the substrate of flat-embedded cells. Sections were collected until all of the cells were completely sectioned from their lower (adhesive) to their upper (nonadhesive) surfaces. No attempts were made to collect sections in sequence as they were cut from the block face. Sections were mounted on 200 mesh Formvar-carbon-coated grids and stained. Microfilament bundles were counted by observing the fluorescent screen through binoculars at a setting of × 10,000 on a Philips 201C electron microscope.
†A cell profile is defined as each cell seen in a thin section. Therefore, one thin section usually had several cell profiles and different thin sections contained different regions of the same cells.

Organization and Distribution of Microfilament Bundles in Normal Mouse 3T3 Cells and Their SV40 Virus-Transformed Derivatives

Growing cultures of the mouse 3T3 line contain many well-spread cells with abundant stress fibers (3, 8, 16, 21, 30–31). Other cells in growing populations contain no obvious stress fibers. As in 9-cell cultures these are usually less extensively spread cells many of which probably represent cells rounding up to enter mitosis and respreading following cytokinesis (13). SV101 cells appear to be significantly smaller than 3T3 cells when viewed by light microscopy. However, this may be related to their inability to adhere to and flatten on solid substrates to the same extent as 3T3 cells, rather than an actual difference in cytoplasmic volume. In addition, SV101 cells possess an altered morphology that gives many of them a spindle-shaped appearance and exhibit extensive overlapping even in subconfluent cultures (Figs. 21A and 21B).

Direct observation of living SV101 cells with phase and Nomarski optics rarely reveals stress fibers. These can only be resolved in the few extensively spread cells that can be found in all growing cultures. It is possible that the inability to distinguish stress fibers in living SV101 cells is related to altered adhesive properties that prevent them from spreading as extensively as 3T3 cells. Once again, an analogous situation can be seen in the early stages of spreading of 3T3 cells. For example, 30 min following trypsinization and replating, 3T3 cells are partially spread and stress fibers are not apparent in any of the cells (Fig. 22A).

Most 3T3 cells in growing cultures contain fluorescent stress fibers following preparation for myosin antibody localization and FS-1 (Fig. 23A). There are also 3T3 cells that do not contain obvious fluorescent stress fibers (Figs. 23B, 23C). These cells are either partially spread or dividing. Similarly, freshly trypsinized and replated 3T3 cells show no fluorescent stress fibers when fixed at 15–30 min following plating (Fig. 22B). These observations substantiate those made on 9 and RE cells; the visibility of fluorescent stress fibers depends on the degree of cell spreading. SV101 cultures contain fewer cells with obvious fluorescent stress fibers (Fig. 24A). In general, stress fibers are more difficult to

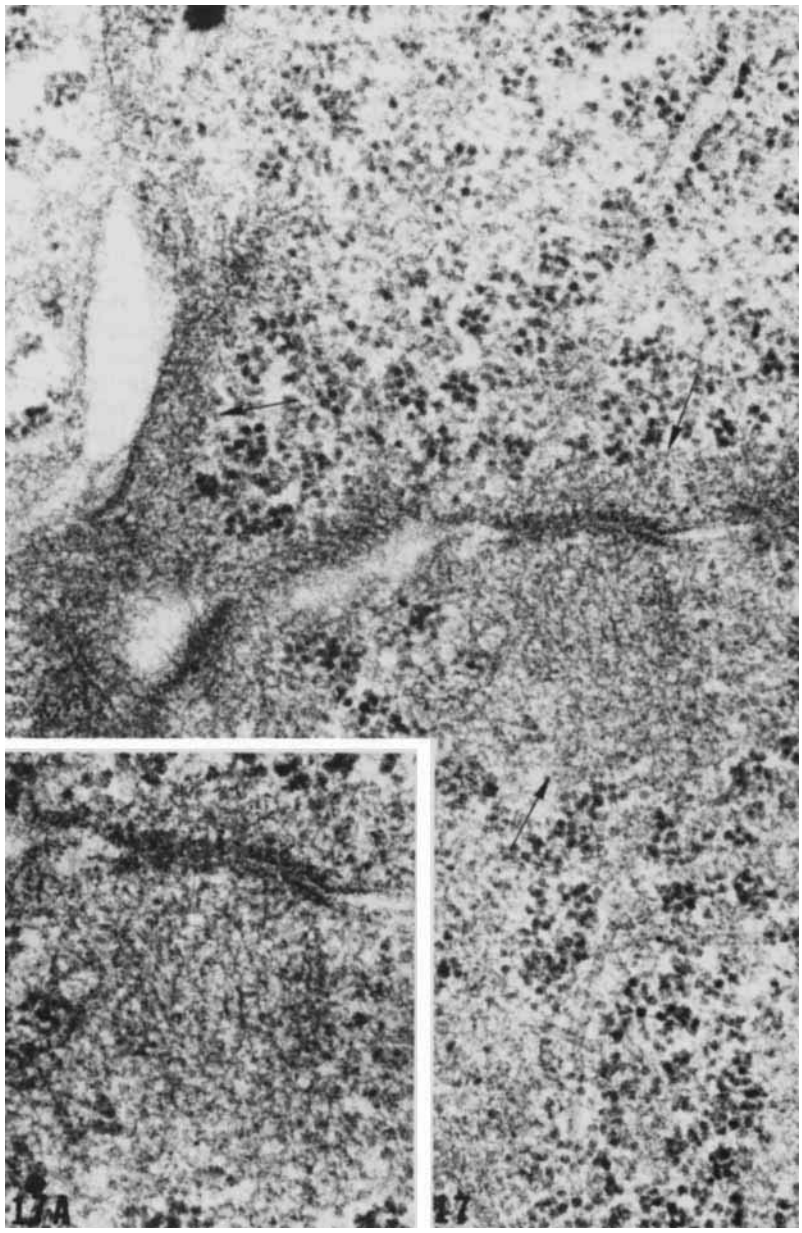

Fig. 17. Electron micrograph of a thin section through the surface of adjacent 14b cells obtained from a flat-embedded preparation of a growing culture. Microfilament meshworks are found subjacent to the plasma membrane (arrows). A) Higher magnification of one of the regions in 17. 17) × 60,000; A) × 76,500.

see in these transformants due to an increase of general fluorescence relative to that seen in 3T3 cells (Fig. 24B). There are also many cells (for example, cells in mitosis, cells in process of respreading following cytokinesis, etc.) without stress fibers (Fig. 24C).

Attempts were made to quantitate the number of cells containing fluorescent stress fibers following myosin antibody treatment in both SV101 and 3T3 cultures. The results

based on the observations of six individuals are presented in Table II. The variability in both the number of cells counted per observer and the number of cells containing fluorescent stress fibers indicates the subjectivity of this type of analysis. This is especially the case since the same photomicrographs were counted by each observer (Table II). In spite of these discrepancies, most of the observers found nearly twice as many fluorescent fiber-containing cells in the 3T3 preparation as those found in the SV101 preparations.

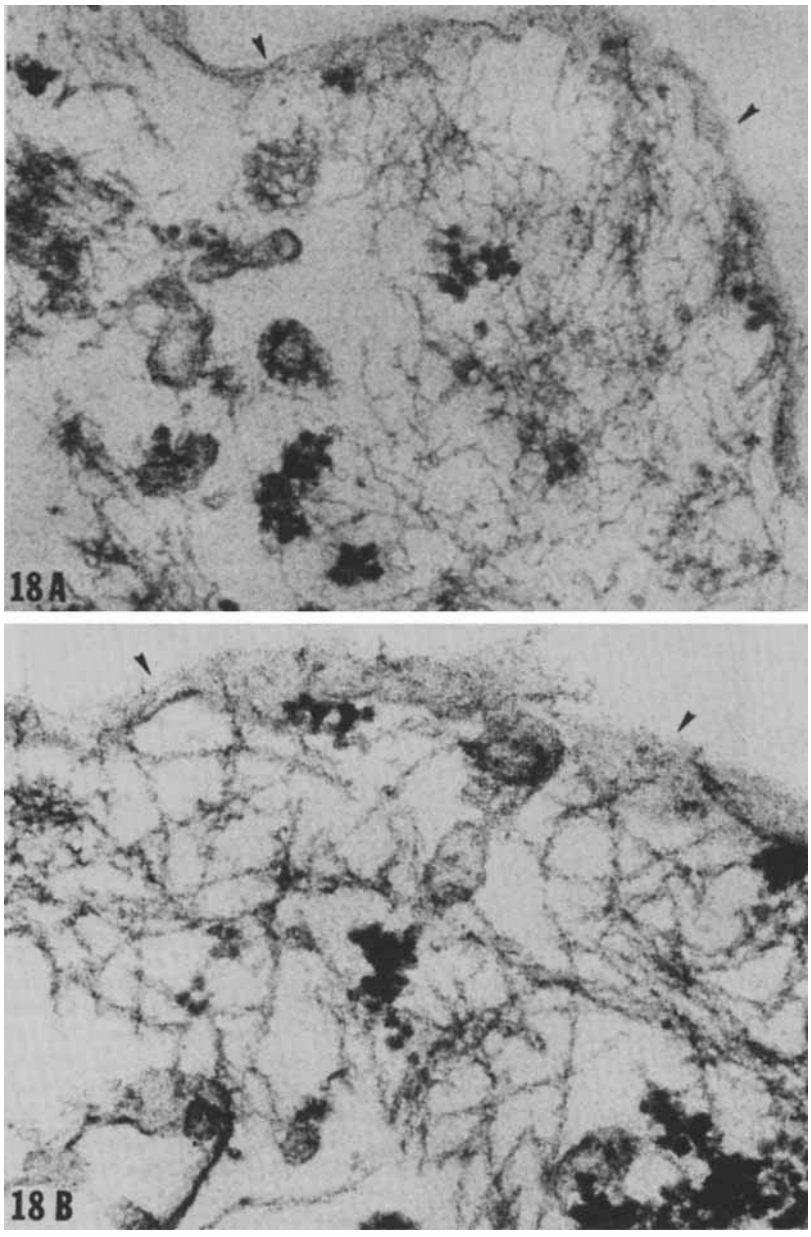

Fig. 18. Submembranous microfilament meshworks following glycerination of 14b cells (A) and following glycerination and HMM binding (B). Arrows point to the remnants of the plasma membrane. A and B) × 99,000.

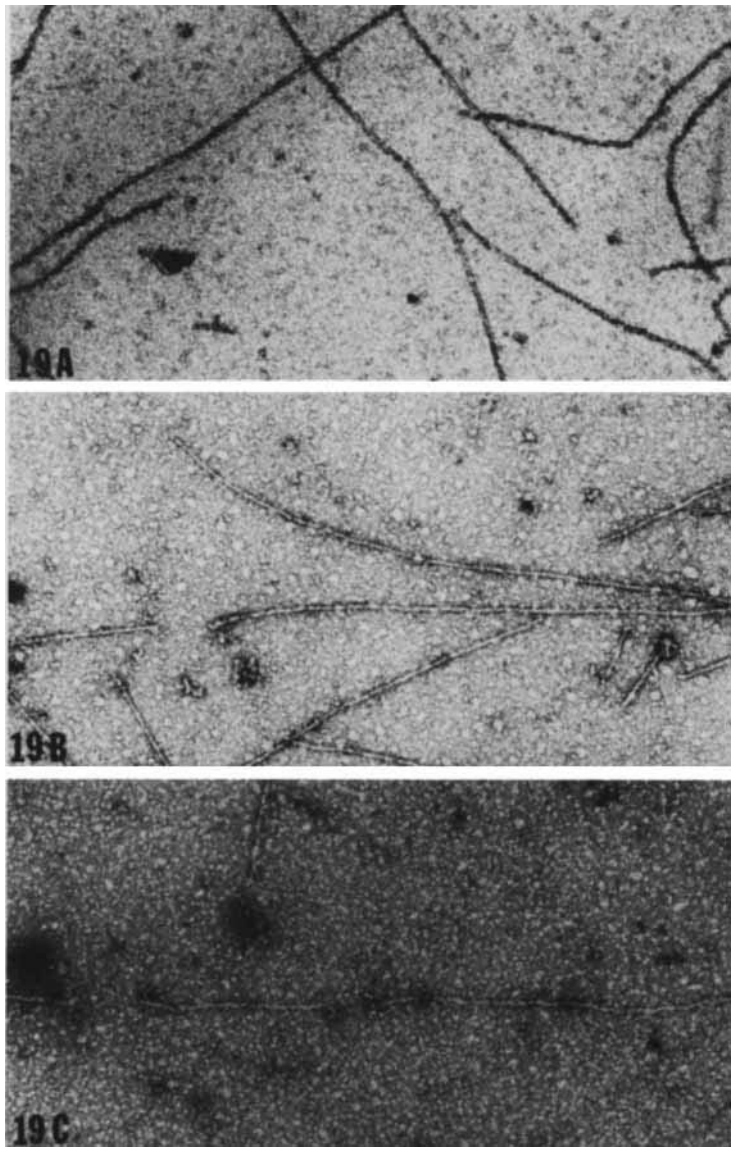

Fig. 19. Rabbit skeletal muscle actin was extracted from an acetone powder (personal communication, Dr. D. Hartshorne) and shown to be free of regulatory proteins and contaminants by SDS-polyacrylamide gel electrophoresis (39). The actin was then depolymerized by dialysis vs 2×10^{-4} M $CaCl_2$, 2×10^{-4} M ATP, and 5×10^{-3} M Tris-HCl, pH 8.0, polymerized by raising the KCl and phosphate concentrations to 0.1 M and 0.01 M, respectively, and applied to Formvar-carbon-coated copper grids at a concentration of 0.1 mg/ml. The grids were either (A) rinsed with PBS, (B) incubated 30 min with 1% glutaraldehyde in PBS and then rinsed, or (C) incubated 30 min with 1% glutaraldehyde, rinsed, incubated 15 min with 1% osmium tetroxide in PBS, and rinsed. All samples were finally stained with 1% uranyl acetate in water. Actin remained fibrous after fixation, although treatment with osmium detroxide induced slightly wavy filament structures in some instances. A, B, and C) × 72,000.

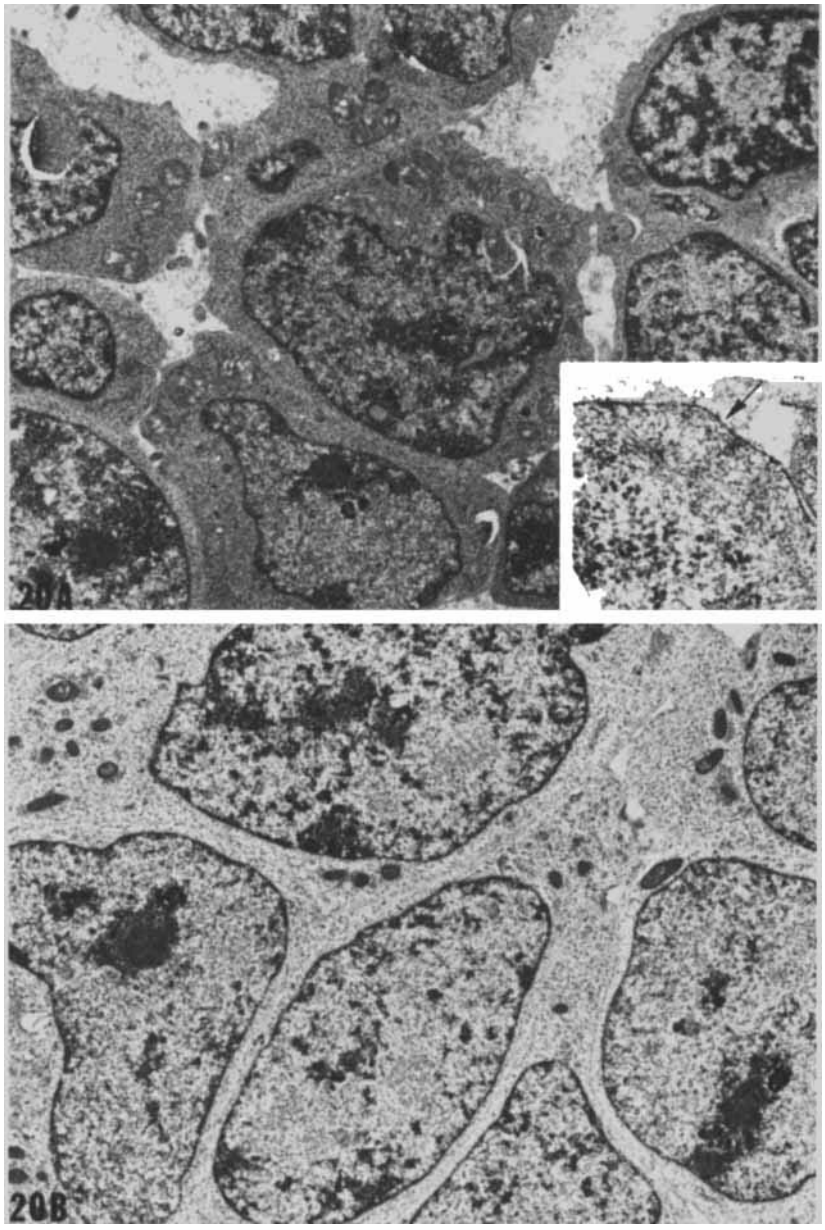

Fig. 20. A. Low-magnification electron micrograph of cells within a 14b-induced tumor. Note resemblance to 14b cells grown in high density culture (B). Insert shows a portion of tumor cell surface and cortical meshwork of microfilaments (arrow). A) × 6,160; insert, × 42,400; B) × 4,960.

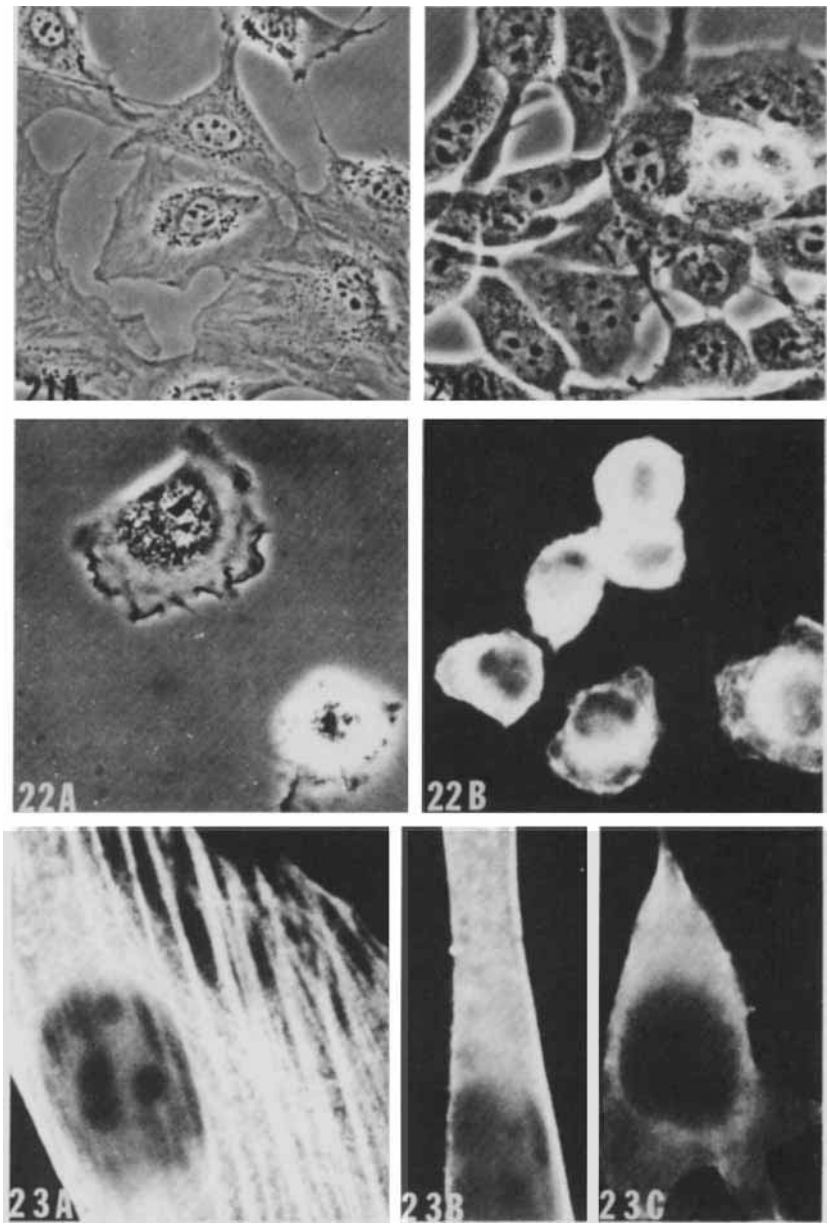

Fig. 21. A. Living 3T3 cells. Note shape and tendency not to overlap extensively. B. Living SV101 cells showing extensive overlapping. Phase contrast; A) × 300; B) × 384.

Fig. 22. A. Living 3T3 cells observed 30 min following plating. B. 3T3 cells prepared by the myosin antibody procedure 30 min after plating. A) Phase contrast, × 480; B) epifluorescence, × 480.

Fig. 23. A–C. Three different 3T3 cells from the same subconfluent coverslip prepared by the myosin antibody technique. Note variability in the expression of fluorescent stress fibers. Epifluorescence, A) × 1,200; B) × 1,200; C) × 1,120.

Ultrastructural studies of both 3T3 cells and SV101 cells demonstrate that microfilament bundles are abundant in both types of cells (Figs. 25, 26). In support of this observation, microfilament bundles were counted in two sets of thin sections of 3T3 cells and SV101 cells. A total of 2,480 SV101 cell profiles were counted and a mean number of 13.9 bundles/cell profile was obtained. For 3T3 cells, 1,261 cell profiles were counted and the mean number of bundles per cell profile was 13.6 (Table III). There was a large variability in the mean number of microfilament bundles seen in the thin sections on one grid relative to another grid obtained from the same block. The range for the 3T3 grids observed was 0–44 microfilament bundles/grid and for the SV101 grids the values ranged

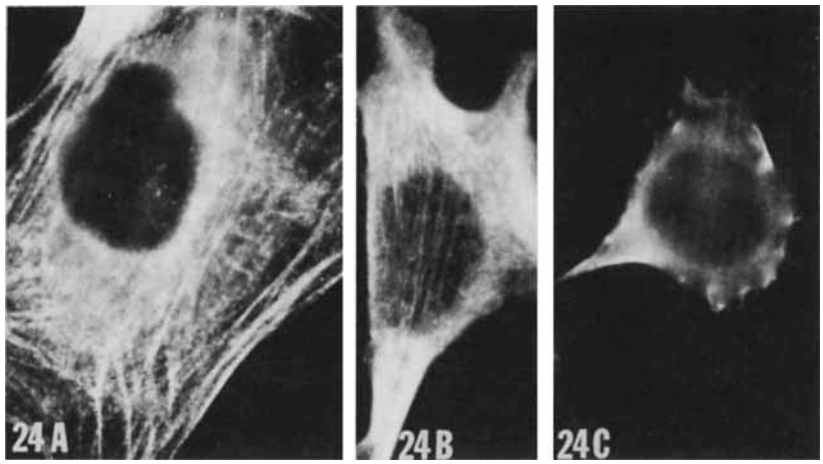

Fig. 24. A–C. Three different SV101 cells from the same subconfluent coverslip prepared by the myosin antibody technique. Epifluorescence, A) × 1,120; B) × 960; C) × 800.

TABLE II. Comparison of Fluorescent Stress Fibers Seen in SV101 and 3T3 Cells*

	SV101			3T3		
Observer	Total no. cells observed	Total no. cells with fluorescent stress fibers	Percent cells with fluorescent stress fibers	Total no. cells observed	Total no. cells with fluorescent stress fibers	Percent cells with fluorescent stress fibers
1	268	82	31	476	319	67
2	333	115	35	483	358	74
3	340	125	37	490	384	78
4	353	153	43	517	415	80
5	299	134	45	493	442	90
6	382	258	68	557	522	94
Mean	329	145	43	503	407	81

*Random microscope fields were photographed using epifluorescence optics with a × 40 Neofluor objective (N.A. 0.75). The negatives obtained were printed at a final magnification of × 1,232 and were given a code number so that the observers did not know which cell type they were studying. In this manner each observer studied 27 fields of SV101 and 43 fields of 3T3 and scored them for both total number of cells and total number of cells containing fluorescent stress fibers. The cells utilized for these observations were grown on glass coverslips and processed for indirect immunofluorescence with myosin antibody.

from 1 to 20 microfilament bundles/grid. The reason for this variability appears to be the fact that microfilament bundles are not distributed uniformly throughout the cells. This is demonstrated in Table IV, which contains data obtained from counting microfilament bundles in one set of 3T3 and one set of SV101 thin sections. The sections were collected and mounted on grids in sequence so that grid No. 1 contained sections in the region of cell-substrate contact and grid Nos. 6 and 7 contained sections near the nonadhesive surface. The counts demonstrate that the majority of microfilament bundles in both cell types are displaced towards the region of cell-substrate contact. However, in 3T3 cells very few microfilament bundles were seen towards the middle and upper surfaces. In contrast, a few microfilament bundles were found distributed deeper in the cytoplasm of SV101 cells (Table IV; see also Fig. 26).

3T3 cells that had been fixed and embedded at 30 min following plating were analyzed for the presence of microfilament bundles. The data (Table V) demonstrate that

TABLE III. Microfilament Bundles in Sets* of Thin Sections of 3T3 and SV101 Cells

Cell type	Total no. of cell profiles* per set of thin sections	Total no. of microfilament bundles per set of thin sections	Mean no. of microfilament bundles per cell profile
3T3	593	9,367	15.8
3T3	668	7,838	11.7
SV101	1,655	28,079	17.0
SV101	825	6,307	7.6

*See Table I for explanation.

TABLE IV. Distribution of Microfilament Bundles in 3T3 and SV101 Cells*

Cell type	Grid no.	No. of cell profiles per grid	No. of microfilament bundles per grid	Mean no. of microfilament bundles per cell profile
3T3	1	77	2,084	27.1
	2	137	2,609	19.0
	3	233	2,507	11.0
	4	153	570	3.7
	5	38	5	0.1
	6	22	0	0
SV101	1	183	2,687	14.7
	2	153	1,092	7.1
	3	234	1,575	6.7
	4	134	623	4.6
	5	70	208	3.0
	6	39	99	2.5
	7	12	23	1.9

*Sets of thin sections made parallel to the substrate of flat-embedded cells were prepared and mounted in sequence so that grid No. 1 contained sections from the region of cell-substrate adhesion and grid Nos. 6 or 7 contained sections from the nonadhesive (upper) cell surface. Following staining, microfilament bundles were counted at × 10,000 through the binoculars of a Philips 201C electron microscope.

appreciable numbers of microfilament bundles are seen adjacent to the adhesive cell surface in the early stages of spreading. This finding is not in concert with the fluorescence observations, that is, stress fibers are not seen in early stages of cell spreading following trypsinization and replating.

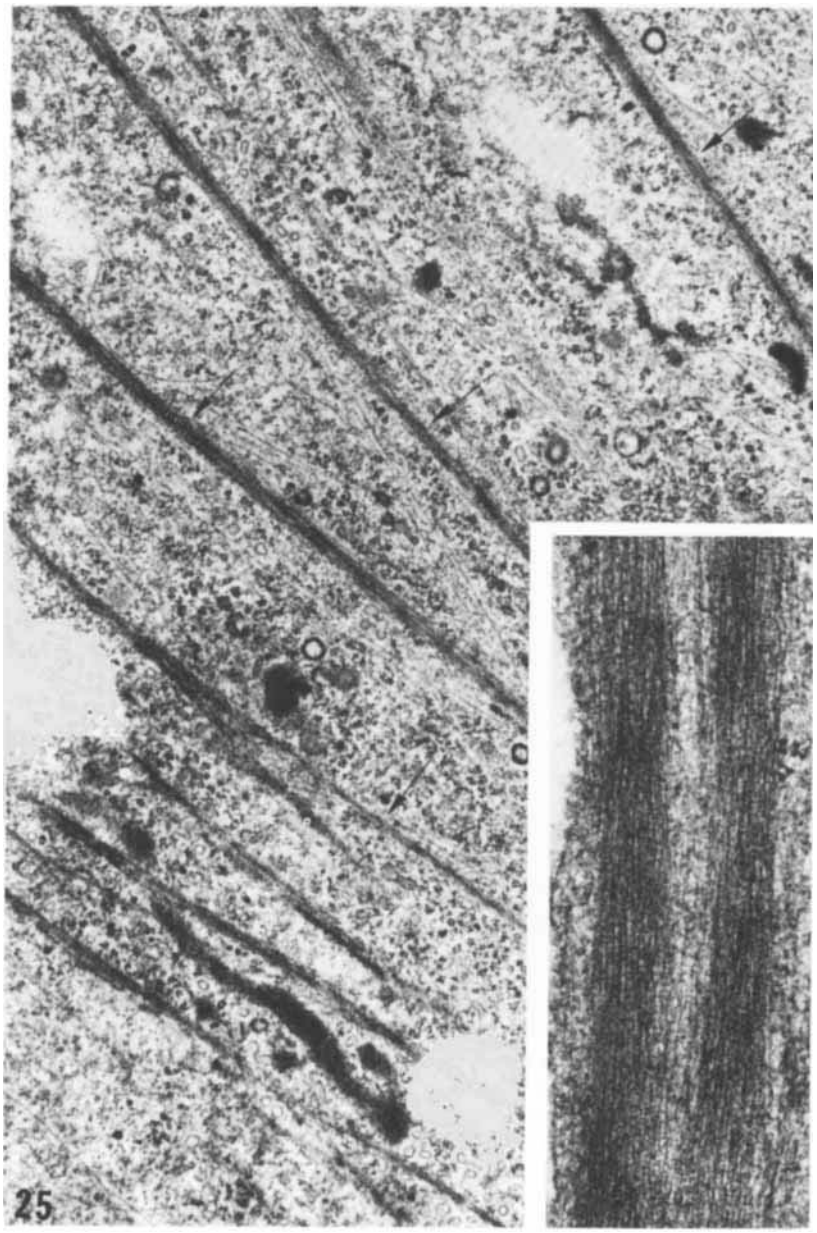

Fig. 25. Electron micrograph of a thin section of a 3T3 cell through the cell cortex adjacent to the region of cell-substrate contact. Microfilament bundles are seen at low magnification (arrows) and a pair are seen at higher magnification (insert), × 15,340; insert, × 49,720.

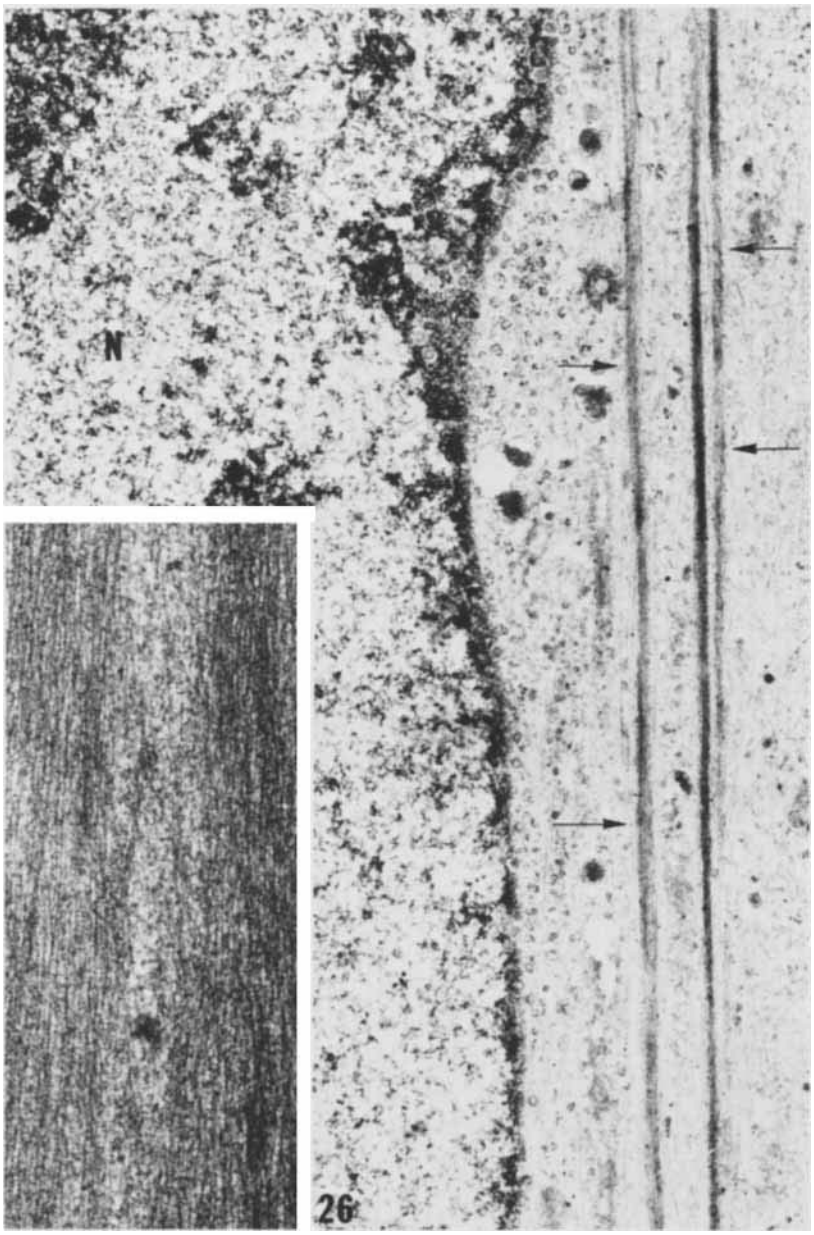

Fig. 26. Electron micrograph obtained from a thin section of an SV101 cell through a cytoplasmic region not immediately adjacent to cell-substrate contact. The nucleus is present (N) and microfilament bundles are seen at low magnification (arrows) and at higher magnification (insert), × 15,340; insert, × 49,720.

An indication of the number of cells containing microfilament bundles in growing cultures of the 3T3 and SV101 lines was obtained by determining the number of cell profiles containing microfilament bundles on the first two grids of a set of thin sections (collected in sequence as described in Table IV). The data in Table VI demonstrate that ~ 95% of the cell profiles observed in SV101 sections and 100% of the cell profiles

TABLE V. Microfilament Bundles in 3T3 Cells During the Early Stages of Cell Spreading*

Grid no.	No. of cell profiles	No. of microfilament bundles	Mean no. of microfilament bundles per cell profile
1	105	1,252	11.9
2	162	1,013	6.3
3	204	805	3.9
4	120	100	0.8
5	127	51	0.4
6	93	6	0.1
7	57	3	0.1
8	32	0	0
9	17	0	0
10	9	0	0
11	0	0	0

*See footnote at bottom of Table IV for details. The increased number of grids containing thin sections (relative to those obtained in Table IV) reflects the fact that the upper cell surface is much further away from the substrate during early spreading.

TABLE VI. Estimate of the Number of Cells Containing Microfilament Bundles in 3T3 and SV101 Cultures*

Cell type	Grid no.	No. of cell profiles	No. of cell profiles containing microfilament bundles
SV101	1	110	102
	2	269	259
3T3	1	94	94
	2	166	166

*The first two grids of sets of thin sections which were made parallel to the substrate of flat-embedded cells and collected in sequence.

observed in 3T3 sections contained microfilament bundles. One possible error in these calculations is the probable omission of some dividing cells that usually pull away from the substrate and therefore may not appear in the thin sections used for this analysis. However, this error is probably small since there are many fewer mitotic cells than interphase cells.

It was necessary to consider whether the thickness of microfilament bundles differed in 3T3 and SV101 cells, in order to help evaluate the discrepancies that exist between the light microscopic and electron microscopic images of these two cell types. Measurements of microfilament bundle thickness were made from electron micrographs of 3T3 and SV101 cells. The results of these measurements are displayed as a histogram in Fig. 27. The data show that there is a wide range of thicknesses as determined from thin-sectioned cells. The mean diameter of 3T3 microfilament bundles is 0.22 μm and of SV101 microfilament bundles is 0.19 μm. The results of a Student's t test comparing these two sets of data indicate that there is little difference between the two sets of measurements ($t = 1.519$; degrees of freedom = 329; $p < 0.1$). However, the range of measurements obtained for 3T3 cells is much broader; thicker microfilament bundles were seen relative to those found in

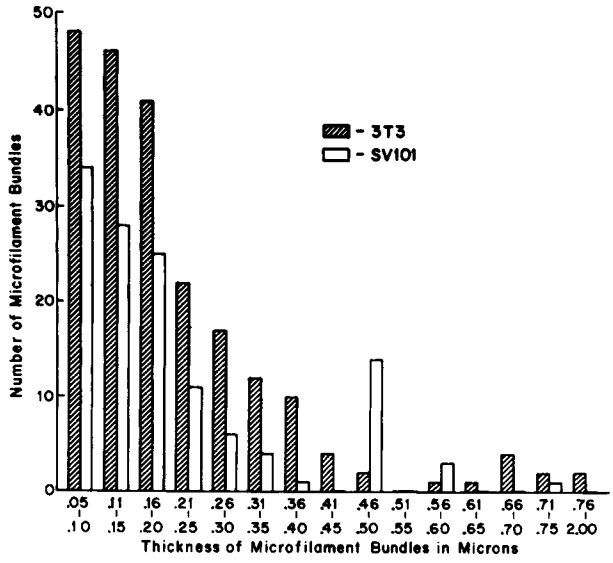

Fig. 27. Microfilament bundle thickness measurements were obtained from fixed flat-embedded growing cultures of 3T3 and SV101 cells. Grids containing thin sections of these preparations were scanned from left to right and the first 16 cell profiles seen to contain microfilament bundles were photographed at × 20,000. This was done twice for each cell type utilizing different thin sections in each instance. Thus a total of 32 electron micrographs were used for each set of measurements. The measurements were made directly on prints of these micrographs at a final magnification of × 60,000. Individual microfilament bundles varied in thickness along their length, but only the thickest regions were used for the measurements.

SV101 cells. Bundles up to 2 μm thick have been measured in this study and elsewhere (16). Thus many of the microfilament bundles seen by electron microscopy could account for the stress fibers seen by light microscopy.

DISCUSSION

The three types of normal cells analyzed in this study possess similar morphological properties. Growing cultures of each cell type contain a subpopulation of extensively spread cells in which stress fibers are easily detected. These stress fibers correspond to actin-like microfilament bundles detected by electron microscopy. However, partially spread cells contain microfilament bundles that do not appear as obvious stress fibers. This is most clearly demonstrated in cells that are in the early stages of spreading following trypsinization and replating. In this case, no stress fibers are seen in living cells or cells prepared by the myosin antibody and FS-1 or FHMM procedures. However, electron microscopy proves that significant numbers of microfilament bundles are present in these cells. These results indicate that the fluorescence observations are most useful in determining the intracellular localization and organization of actomyosin-like structures in well-spread cells but not in the partially spread cells often seen in growing cultures.

The two types of virus-transformed cell lines are distinguished by significant morphological alterations. These changes in morphology may be related to a loss of adhesive properties and a general inability to spread as extensively as normal cells when

attached to solid substrates. In both cases, these morphological alterations are accompanied by a general loss of obvious stress fibers as determined by the light microscopic techniques. The most obvious changes take place in the rounded adenovirus transformants (14b cells) in which no stress fibers are seen. The fluorescence procedures reveal only a diffuse peripheral fluorescence in these cells. Ultrastructural analyses confirm these observations, as microfilament bundles are absent in the vast majority of cells. Despite these findings, actin-like protein is present in relatively large amounts in 14b cells and appears to exist primarily as a submembranous meshwork of microfilaments.

In SV40-transformed 3T3 cells (SV101), light microscopic analyses show that most cells do not possess stress fibers, which is in agreement with other studies on similar types of cells (30–32). However, electron microscopy reveals that there are as many microfilament bundles present in the cytoplasm of SV101 cells as in normal 3T3 cells. Most of the microfilament bundles are found in the cortical cytoplasm just beneath the plasma membrane at the adhesive surface of both cell types. However, there appear to be significant numbers of microfilament bundles distributed deeper in the cytoplasm in SV101 cells.

These results demonstrate that the majority of SV101 cells studied by light microscopy do not reflect the number and distribution of microfilament bundles as determined by electron microscopy. This discrepancy does not appear to be due to a significant difference in either the thickness or number of microfilament bundles. Perhaps the intracellular arrangement of microfilament bundles is such that they are not amenable to being resolved as stress fibers by light microscopy. For example, the altered morphology of SV101 cells tends to make them appear more fibroblastic than 3T3 cells. This probably results in microfilament bundles being packed closer together in the long spike-like projections that are characteristic of SV101 cells. Consequently, the distances between individual bundles or stress fibers might be much more difficult to resolve. In contrast, 3T3 cells contain few spike-like projections but do possess broad sheets of cytoplasm. In this instance, similar numbers of microfilament bundles might be more easily resolved as stress fibers due to the fact that they are separated by greater distances. Evidence in support of this possible explanation stems from observations on BHK-21 cells. These cells possess an overall morphology that is similar to that of SV101 cells. BHK-21 cells contain many microfilament bundles (2–3) but rarely display stress fibers. However, treatment with colchicine induces the cells to alter their shape coincident with a loss of microtubules. The resulting cells become more flattened and appear similar to 3T3 cells. Such colchicine-treated BHK-21 cells display impressive arrays of stress fibers that can be accounted for by the microfilament bundles seen in electron microscope preparations (8, 12, 34). This phenomenon is completely reversible and when colchicine is removed, the cells rapidly reacquire their fibroblastic shape, and once again stress fibers are not apparent. Therefore, the differences between 3T3 and SV101 cells as seen by light optical methods appear to be due to the intracellular distribution, localization, and packing of microfilament bundles and not to gross alterations in the number of microfilament bundles.

The results of this study emphasize the importance of combining light and electron optical procedures, and in some instances biochemical procedures, in determining the organization and distribution of microfilament bundles, as well as other less organized arrays of microfilaments. It has been suggested by several investigators that the fluoresence techniques provide a rapid and overall impression of the differences in distribution and organization of actin and myosin in normal and transformed cells. This study demonstrates that significant errors in interpretation can result when fluorescence procedures are used exclusively.

Very little is known regarding the specific mechanisms by which actomyosin-like contractile proteins function in nonmuscle mammalian cell motility. It is therefore extremely difficult to evaluate the significance of the differences seen between normal cells and their DNA virus-transformed derivatives. However, there is sufficient circumstantial evidence that microfilament bundles, possibly in conjunction with microtubules and 10 nm filaments (2, 12, 13), function in several motile phenomena associated with the surface of mammalian cells grown in vitro. These phenomena include cell spreading and shape formation (3, 12, 13), locomotion (8, 14–19), contact inhibition (7, 8) and cytokinesis (9, 10). Thus the absence of microfilament bundles in 14b cells corresponds with their inability to spread and engage in normal locomotory behavior (29). More specifically, 14b cells do not exhibit the contact-mediated assembly of microfilament bundles thought to be important in and prerequisite to normal cell shape formation and locomotion (3, 8). Since this contact-mediated assembly process appears to involve, at least in part, a conversion of microfilament meshworks into microfilament bundles, it is likely that 14b cells are incapable of carrying out this conversion process under normal culture conditions.

The relevance of the findings in SV101 cells is more elusive as there are no obvious changes in the number of microfilament bundles relative to 3T3 cells. One possible alteration lies in the distribution of microfilament bundles. In SV101 cells there appear to be more bundles located in areas away from the cortical cytoplasm adjacent to cell-substrate contacts. This may be related to the ability of SV101 cells to spread and perhaps migrate over and under each other to form their characteristic overlapping arrays.

At the present time there is no way of knowing whether or not the changes in microfilaments seen in adenovirus-5- and SV40-transformed cells are direct or indirect consequences of the expression of viral genes that become incorporated into the host cell genome. Conceivably any specific virus-induced chemical or topographical alteration in the glycocalyx could lead to alterations in adhesive properties, which indirectly could alter the distribution and organization of many cytoplasmic structures including microfilaments. Even though the changes seen in microfilament organization may be indirect, they could significantly alter the function of the cytoplasmic contractile machinery, which in turn could cause the aberrant behavior patterns characteristic of tumorigenic cells. Thus the exact relationship between the ultrastructural alterations seen in microfilaments and the tumorigenicity of virus-transformed cells remains to be established.

ACKNOWLEDGMENTS

We wish to thank Dr. James Williams for kindly providing the 14b tumors. We also thank Bonnie Chojnacki, Anne Goldman and Anne Bushnell for the excellent technical assistance. This work was supported by grants from the National Cancer Institute (No. 5 RO1 CA17210-02) and the American Cancer Society.

REFERENCES

1. Buckley, I. K., and Porter, K. R., Protoplasma 64:24 (1967).
2. Goldman, R. D., and Follett, E. A. C., Exp. Cell Res. 57:263 (1969).
3. Goldman, R. D., J. Histochem. and Cytochem., 23:529 (1975).
4. Ishikawa, H., Bischoff, R., and Holtzer, H., J. Cell Biol. 43:312 (1969).
5. Mooseker, M. S., and Tilney, L. G., J. Cell Biol. 67:725 (1975).
6. Pollard, T. D., and Weihing, R., CRC Critical Reviews of Biochem. 2:1 (1974).
7. Heaysman, J., In "Locomotion of Tissue Cells," Ciba Found. Symp. 14:185 (1973).

8. Goldman, R. D., Schloss, J. A., and Starger, J. M., in "Cell Motility," R. Goldman, T. Pollard, and J. Rosenbaum (eds.). Cold Spring Harbor Series on Animal Cell Proliferation (in press).
9. Schroeder, T. E., Zeit. für Zell Forsch. 109:431 (1970).
10. Schroeder, T. E., Proc. Nat. Acad. Sci. 70:1688 (1973).
11. Albrecht-Buehler, G., and Goldman, R. D., Exp. Cell Res. 97:329 (1976).
12. Goldman, R. D., and Knipe, D., Cold Spring Harbor Symp. Quant. Biol. 37:523 (1973).
13. Goldman, R. D., Berg, G., Bushnell, A., Chang, C-M., Dickerman, L., Hopkins, N., Miller, M. L., Pollack, R., and Wang, E., in "Locomotion of Tissue Cells," Ciba Found. Symp. 14:83 (1973).
14. Wessells, N. K., Spooner, B. S., Ash, J. F., Bradley, M. O., Luduña, M. A., Taylor, E. L., Wrenn, J. T., and Yamada, K. M., Science 171:135 (1971).
15. Wessells, N. K., Spooner, B. S., and Ludueña, M. A., in "Locomotion of Tissue Cells," Ciba Found. Symp. 14:53 (1973).
16. Goldman, R. D., Lazarides, E., Pollack, R., and Weber, K., Exp. Cell Res. 90:333 (1975).
17. Spooner, B. S., Yamada, K. M., and Wessells, N. K., J. Cell Biol. 49:595 (1971).
18. Spooner, B. S., Ash, J. F., Wrenn, J. T., Frater, R. B., and Wessells, N. K., Tiss. and Cell 5:37 (1973).
19. Yamada, K. M., Spooner, B. S., and Wessells, N. K., J. Cell Biol. 49:614 (1971).
20. Lazarides, E., and Weber, K., Proc. Nat. Acad. Sci. 71:2268 (1974).
21. Weber, K., and Groeschl-Stewart, U., Proc. Nat. Acad. Sci. 71:4561 (1974).
22. Fujiwara, K., and Pollard, T., J. Cell Biol 67:125a (1975).
23. Lazarides, E., J. Histochem. and Cytochem. 23:507 (1975).
24. Lazarides, E., J. Cell Biol. 65:549 (1975).
25. Lazarides, E., J. Cell Biol. 68:202 (1976).
26. Lazarides, E., and Burridge, K., Cell 6:289 (1975).
27. McNutt, N. S., Culp, L. A., and Black, P. H., J. Cell Biol. 50:691 (1971).
28. McNutt, N. S., Culp, L. A., and Black, P. H., J. Cell Biol. 56:412 (1973).
29. Goldman, R. D., Chang, C., and Williams, J. F., Cold Spring Harbor Symp. Quant. Biol. 39:601 (1974).
30. Weber, K., Lazarides, E., Goldman, R. D., Vogel, A., and Pollack, R., Cold Spring Harbor Symp. Quant. Biol. 39:363 (1974).
31. Pollack, R., Osborn, M., and Weber, K., Proc. Nat. Acad. Sci. 72:994 (1975).
32. Pollack, R., and Rifkin, D., Cell 6:495 (1975).
33. Williams, J. F., Nature 243:162 (1973).
34. Goldman, R. D., J. Cell Biol. 51:752 (1971).
35. Szent-Györgyi, A., "Chemistry of Muscular Contraction," Academic Press, 2nd ed., (1951).
36. Weeds, A. G., and Taylor, R. S., Nature 257:54 (1975).
37. Pollard, T. D., Shelton, E., Weihing, R., and Korn, E., J. Mol. Biol. 50:91 (1970).
38. Aronson, J., J. Cell Biol. 26:293 (1965).
39. Fairbanks, G., Steck, T. L., and Wallach, D. F. H., Biochem. 10:2606 (1971).
40. Locke, M., and Krishnan, N., J. Cell Biol. 50:550 (1971).
41. Reynolds, E. S., J. Cell Biol. 17:208 (1963).
42. Szamier, P., Pollard, T., and Fujiwara, K., J. Cell Biol. 67:424a (1975).
43. Sanger, J. W., Proc. Nat. Acad. Sci. 72:1913 (1975).